XVI CONGRESSO BRASILEIRO DE ENGENHARIA MECÂNICA
16th BRAZILIAN CONGRESS OF MECHANICAL ENGINEERING

MODELING OF PLATE HEAT EXCHANGERS WITH GENERALIZED CONFIGURATIONS

Jorge Andrey Wilhelms Gut
Department of Chemical Engineering - University of São Paulo
Av. Prof. Luciano Gualberto, trav. 3, 380 / São Paulo - SP / 05508-900 / BRAZIL
andrey@lscp.pqi.ep.usp.br

José Maurício Pinto
Department of Chemical Engineering - University of São Paulo
Av. Prof. Luciano Gualberto, trav. 3, 380 / São Paulo - SP / 05508-900 / BRAZIL
jompinto@usp.br

Abstract. *A mathematical model is developed for the simulation of gasketed plate heat exchangers, operating in steady state, with a general configuration. The main purposes of this model are to study the influence of the configuration on the equipment performance and to further develop a method for optimizing the exchanger configuration. The configuration is defined by six parameters, which are as follows: number of channels, number of passes at each side, fluid locations, feed connection locations and type of channel-flow. The mathematical model is developed through an assembling algorithm, since it is not possible to represent the model explicitly as a function of the six parameters. The resulting system is composed of ordinary differential equations of the boundary value type, which is solved by the finite difference method, using the software gPROMS (Process Systems Enterprise, 2001). The main simulation results are the following: temperature profiles in all channels, thermal effectiveness, distribution of the overall heat transfer coefficient along the exchanger and fluid pressure drops. Examples of heat exchangers with approximately 150 plates yield algebraic models with thousands of equations, which are solved within minutes. Moreover, the assumption of invariant overall heat transfer coefficient is verified.*

Keywords: *plate heat exchanger, mathematical modeling, finite difference method, heat exchanger configuration*

1. Introduction

For being compact, easy to clean, efficient and very flexible, the gasketed plate heat exchanger (PHE) is widely employed in the chemical, food and pharmaceutical process industries. The PHE consists of a pack of gasketed corrugated metal plates, pressed together in a frame (see Fig. 1). The gaskets on the corners of the plates form a series of parallel flow channels, where the fluids flow alternately and exchange heat through the thin metal plates. The gasket design and the closed ports of the plates determine the fluid flow distribution, which can be parallel, series or any of their various possible combinations. The number of plates, flow distribution, type of gaskets and the fluid feed locations characterize the exchanger configuration.

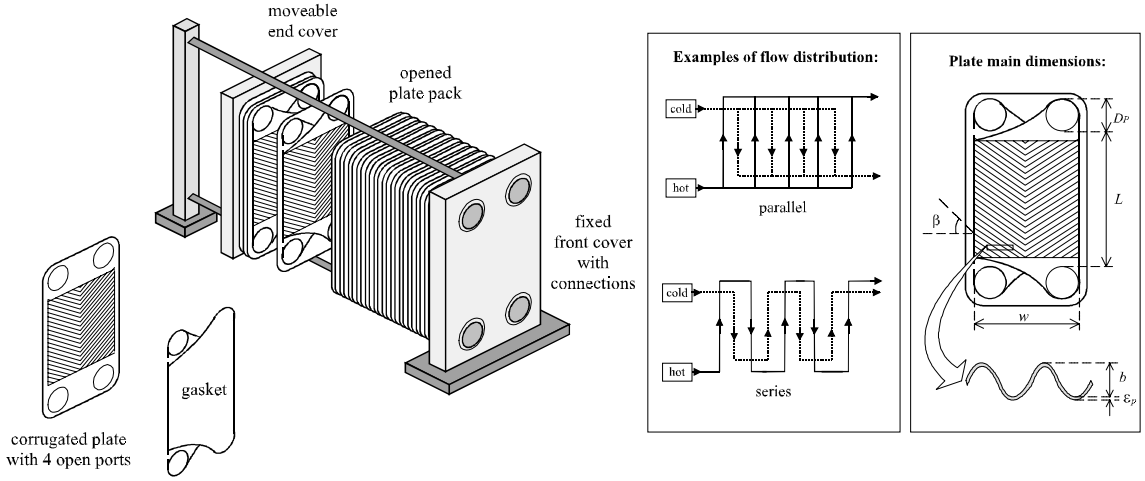

Figure 1. The plate heat exchanger assemblage, examples of flow distributions and plate main dimensions.

The simplified thermal modeling of a PHE in steady state yields a linear system of first order ordinary differential equations, comprising the energy balance for each channel and the required boundary conditions. The main assumptions are as follows: plug-flow inside the channels, constant overall heat transfer coefficient along the exchanger, uniform distribution of flow in the channels, no heat loss and no heat exchange in the flow direction. This basic model was presented by McKillop & Dunkley (1960) for 3 different configurations and also by Masubuchi & Ito (1977), where the

dynamic responses of some usual configurations were studied. In both works, the Runge-Kutta-Gill integration method was used to solve the system of equations.

The integration is non-trivial because the boundary conditions are defined at different extremes of the channel. Approximate solutions were developed by Settari & Venart (1972) in polynomial form, and by Zaleski & Klepacka (1992) in exponential form. Both methods lead to good approximations of the exact solution, but they may not be reliable when there is a large difference between fluid heat capacities.

Kandlikar & Shah (1989b) developed a method to calculate an approximated thermal effectiveness for large exchangers, where the effects of the end plates and of the changes of passes can be neglected. In this case, the exchanger is divided into a group of simpler exchangers that are interconnected, with known effectiveness.

The analytical solution of the system of equations in matrix form was studied by Zaleski & Jarzebski (1973) and Zaleski (1984) for exchangers with series and parallel arrangements. This solution method may lead to numerical problems on the calculation of eigenvalues and eigenvectors, and it is not recommended for large sized exchangers.

Kandlikar & Shah (1989a) and Georgiadis et al. (1998) used the finite difference method for the simulation of PHEs. Kandlikar & Shah (1989a) simulated and compared several configurations. It was verified that higher effectiveness is achieved when the exchanger is symmetrical, with the same numbers of passes for both streams, because the channels that are next to the changes of passes as well as the end channels have a lower effectiveness. However, when the fluids have very different flow rates or heat capacities, a non-symmetrical configuration must be used. In such cases, there is no rigorous design method to select the best configuration, which is made by comparison among the usual configurations from thermal effectiveness and pressure drop viewpoints.

Georgiadis et al. (1998) presented a detailed modeling of a PHE used for milk pasteurization that couples the dynamic thermal model with the protein-fouling model. Three different configurations were compared and the reduction of the overall heat transfer coefficient, caused by the protein adhesion on the plates, was studied. The model was solved with the finite difference method, implemented in the software gPROMS (Process System Enterprise, 2001).

To the authors knowledge there is no rigorous design method for PHEs in the open literature, as there are for the shell-and-tube exchangers (Taborek, 1983). Shah & Focke (1988) have presented a detailed step-by-step design procedure for rating and sizing a PHE, which is however restricted to parallel flow arrangements.

In all of those works, the overall heat transfer coefficient was considered invariable along the exchanger because this assumption brings a great simplification for the solution of the system of equations, linearizing the differential equations of the channel fluid temperatures. However, there may be a considerable variation of the overall coefficient for some cases, such as the series flow arrangement with equal flow rates of the fluids (Buonopane et al, 1963).

The aim of this work is to present a PHE modeling framework that is suitable for any configuration. The purpose of developing such model is to study the influence of the configuration on the exchanger performance and to further develop an optimization method for configuration selection. The first step for the modeling concerns the parameterization of the different configurations, following the work of Pignotti & Tamborenea (1988). The variation of the overall heat transfer coefficient along the exchanger is also studied in this work, with respect to the assumption of a constant value.

Nomenclature

a	*generic model parameter*
A	*effective heat transfer area (m^2)*
b	*channel average thickness (m)*
Cp	*fluid specific heat at constant pressure (J/kg.K)*
D_e	*equivalent diameter of channel (m)*
D_P	*port diameter (m)*
E	*exchanger thermal effectiveness (%)*
f	*Fanning friction factor*
g	*gravitational acceleration ($g = 9{,}8\ m/s^2$)*
G_C	*channel mass velocity ($kg/m^2.s$)*
G_P	*port mass velocity ($kg/m^2.s$)*
h	*convective heat transfer coefficient ($W/m^2.K$)*
k	*fluid thermal conductivity (W/m.K)*
k_P	*plate thermal conductivity (W/m.K)*
L	*effective plate length, measured between ports (m)*
M	*diagonal matrix defined with Eq. (10)*
N	*number of channels per pass*
N_C	*number of channels*
Nu	*Nusselt number*
P	*number of passes*
Pr	*Prandtl number*
R	*fluid fouling factor ($m^2.K/W$)*
Re	*Reynolds number*
s_i	*channel i flow direction parameter ($s_i = +1$ or -1)*
T	*temperature (K)*
U	*overall heat transfer coefficient ($W/m^2.K$)*
w	*effective plate width, measured between gaskets (m)*
W	*fluid mass flow rate (kg/s)*
x	*coordinate, tangential to channel fluid flow (m)*
Y_f	*binary parameter for type of channel-flow*
Y_h	*binary parameter for hot fluid location*
α	*dimensionless variable defined with Eq. (9)*
β	*chevron corrugation inclination angle (degrees)*
ΔP	*fluid pressure drop (Pa)*
ρ	*fluid density (kg/m^3)*
ε	*maximum deviation for calculated thermal effectiveness*
ε_P	*thickness of metal plate (m)*
ϕ	*parameter for feed connection relative location*
Φ	*enlargement factor of plate*
η	*dimensionless coordinate, tangential to channel fluid flow*
μ	*fluid viscosity (Pa.s)*
θ	*dimensionless fluid temperature*

Subscripts

c	*cold fluid*
h	*hot fluid*
i	*generic element i*
in	*fluid inlet*
max	*maximum value*
min	*minimum value*
out	*fluid outlet*
w	*at the plate wall*

Superscripts

I	*side I of exchanger*
II	*side II of exchanger*

2. Configuration Characterization

The configuration of a PHE is defined by the information that allows the detailing of the equipment assemblage, including the connections on the fixed and moveable covers, the closed and open ports in each plate and the type and position of each gasket. To characterize such configurations, six distinct parameters are used: N_C, P^I, P^{II}, ϕ, Y_h and Y_f. These parameters are defined with details in Tab. (1).

Table 1. Characterization of the six configuration parameters.

Parameter description	Illustrative figure
N_C : Number of Channels The space comprised between two plates is a channel, and the PHE can be represented by a row of channels, numbered from 1 to N_C. The odd-numbered channels belong to side I, and the even-numbered ones belong to side II (as an analogy to the "tube" and "shell" sides in a shell-and-tube exchanger). N_C^I and N_C^{II} are the numbers of channels in each side. If N_C is even, both sides have the same number of channels, otherwise side I has one more channel. Allowable values: 2, 3, 4, 5 …	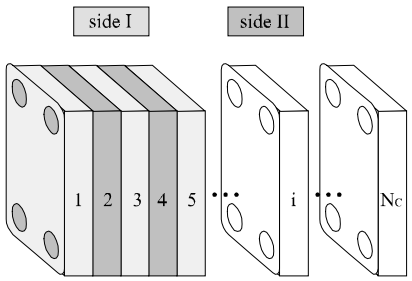
P^I and P^{II} : Number of passes at sides I and II A pass is a set of channels where the stream is split and distributed. For a regular configuration, each side of the PHE is split into passes with the same number of channels per pass (N^I and N^{II}). Passes with different numbers of channels are unusual (Kakaç & Liu, 1998). The relationship between N_C, P^I and P^{II} is given in Tab. (2). Allowable values: from the factorization of N_C^I and N_C^{II} respectively	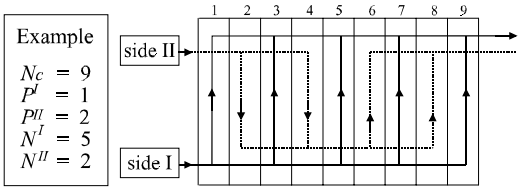
ϕ : Feed connection relative location The feed connection of side I is arbitrarily set in channel 1 at η=0. The relative position of the feed of side II is given by the parameter ϕ, as shown in the diagram (Pignotti & Tamborenea, 1988). The dimensionless length η is not associated with the top and bottom of the PHE, neither channel 1 is associated with the fixed cover. The configuration can be freely rotated or mirrored. Allowable values: 1, 2, 3 and 4	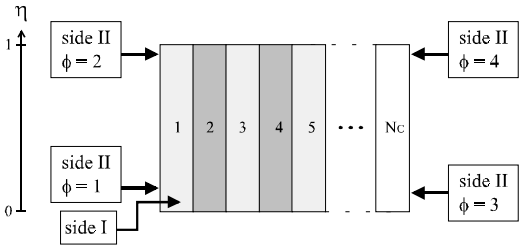
Y_h : Hot fluid location This binary parameter assigns the fluids to the exchanger sides: - if Y_h = 1 : the hot fluid is at side I, and the cold fluid at side II - if Y_h = 0 : the cold fluid is at side I, and the hot fluid at side II	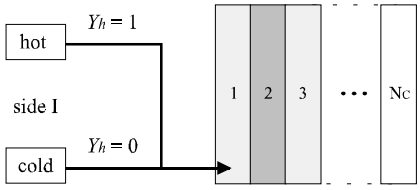
Y_f : Type of flow in channels Y_f is a binary parameter that defines the type of flow inside the channels. As shown in the diagram, the flow can be straight or crossed, depending on the gasket type. The crossed flow avoids the formation of stagnation areas, but the straight flow type is easier to assemble. It is not possible to use both types together. - if Y_f = 1 : the flow is crossed in all channels - if Y_f = 0 : the flow is straight in all channels	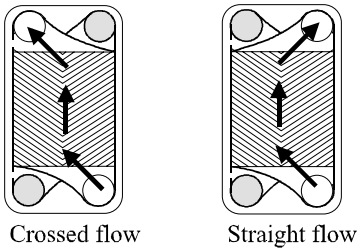

The six parameters can represent any regular configuration. For a fixed number of channels N_C, the five remaining parameters have a known set of allowable values. The combination gives a finite number of possible regular configurations for each value of N_C, as presented in Fig. (2). The disperse pattern is due to the variation of the number of integer factors of N_C^I and N_C^{II} for each value of N_C.

A configuration example is shown in Fig. (3) for illustration. It represents an eight-plate PHE, where the hot fluid in side I (Y_h=1) makes 2 passes (P^I=2) and the cold fluid on side II makes 3 passes (P^{II}=3). In this example, the inlet of

side II is located next to the inlet of side I (ϕ=1) and the type of channel-flow is crossed flow (Y_f=1). The parameter Y_f for type of channel-flow is mostly useful for the exchanger physical construction and it may not be necessary for the simulation since its influence over the convective coefficients and friction factors is usually unknown.

Table 2. Relationship between numbers of channels and passes.

Main equations			
$N_C = N_C{}^I + N_C{}^{II}$	$N_C{}^I = N^I.P^I$	$N_C{}^{II} = N^{II}.P^{II}$	
If N_C is <u>even</u>:		If N_C is <u>odd</u>:	
$N_C{}^I = \frac{N_C}{2}$	$N^I = \frac{N_C}{2.P^I}$	$N_C{}^I = \frac{N_C+1}{2}$	$N^I = \frac{N_C+1}{2.P^I}$
$N_C{}^{II} = \frac{N_C}{2}$	$N^{II} = \frac{N_C}{2.P^{II}}$	$N_C{}^{II} = \frac{N_C-1}{2}$	$N^{II} = \frac{N_C-1}{2.P^{II}}$

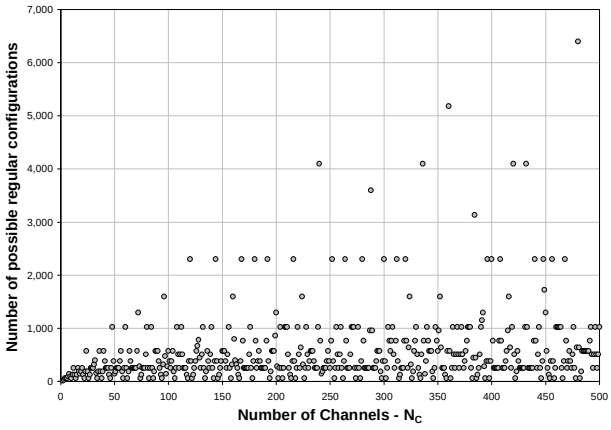

Figure 2. Number of possible regular configurations as a function of the number of channels.

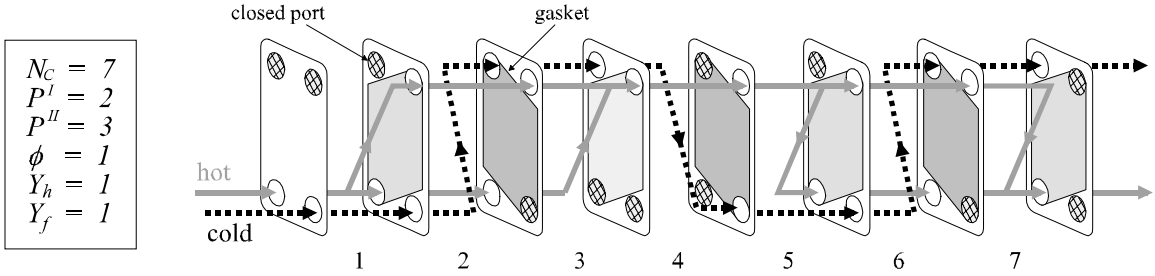

Figure 3. Example of configuration for a PHE with eight plates.

3. Equivalent Configurations

For a given value of number of channels and a fixed type of flow, the existence of equivalent configurations (that have the same thermal effectiveness and pressure drops) is possible. The identification of the equivalent configurations is important to avoid unnecessary simulations. The equivalence occurs due to 3 remarks, as follows:

A1) According to the property of flow reversibility (Pignotti & Tamborenea, 1988), the inversion of the fluid flow direction in both sides does not alter the effectiveness of the PHE.

A2) When there is a single pass in a side, the flow direction is the same in all channels, regardless if the feed is located at the first channel or at the last one.

A3) Simply inverting the direction of η, or numbering the channels in reverse order, may yield to a new set of configuration parameters.

A methodology to detect equivalent configurations is presented in Tab. (3). For each set N_C, P^I, P^{II} and Y_f there are groups of the parameter ϕ that result in equivalent configurations. In the case of an even-numbered N_C, there may be equivalency between Y_h = 0 and Y_h = 1, because sides I and II have the same number of channels and therefore can support the same passes. An example of equivalency between 4 different configurations is shown in Fig. (4).

Table 3. Identification of equivalent configurations for given values of N_C and Y_f.

N_C	(P^I , P^{II})	Groups of equivalent values of ϕ	Reduction in the number of simulations
odd	(1 , 1) ; (1 , odd) ; (odd , 1)	{1 , 3} ; {2 , 4}	50 %
	(1 , even) ; (even , 1)	{1 , 2 , 3 , 4}	75 %
	(odd , odd) ; (even , even)	{1} ; {2} ; {3} ; {4}	0 %
	(odd , even) ; (even , odd)	{1 , 2} ; {3 , 4}	50 %
even	(1 , 1) ; (1 , odd) ; (odd , 1)	{1*h* , 3*h* , 1*c*, 3*c*} ; {2*h* , 4*h* , 2*c* , 4*c*}	75 %
	(1 , even)*h*	{1*h* , 4*h* , 2*c*, 4*c*} ; {2*h* , 3*h* , 1*c* , 3*c*}	75 %
	(even , 1)*h*	{1*h* , 3*h* , 2*c*, 3*c*} ; {2*h* , 4*h* , 1*c* , 4*c*}	75 %
	(odd , odd) ; (even , even)	{1*h* , 1*c*} ; {2*h*, 2*c*} ; {3*h* , 3*c*} ; {4*h* , 4*c*}	50 %
	(odd , even) ; (even , odd)	{1*h* , 2*c*} ; {2*h*, 1*c*} ; {3*h* , 3*c*} ; {4*h* , 4*c*}	50 %

Note: when N_C is even, "h" denotes Y_h = 1 and "c" denotes Y_h = 0. When N_C is odd, all equivalent configurations have the same value for Y_h.

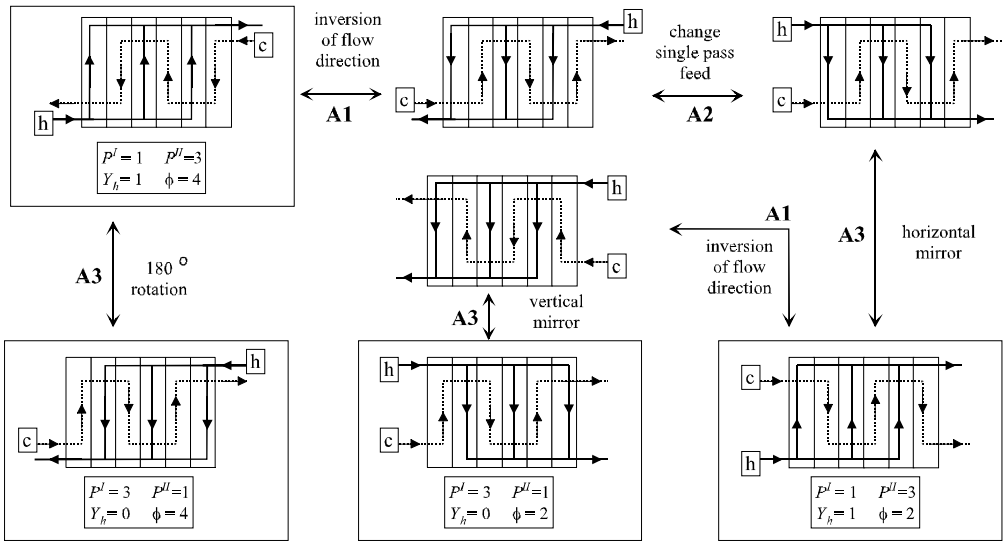

Figure 4. Example of four equivalent configurations with N_C = 6 and Y_f = 1.

4. Modeling of the PHE

The following assumptions were made in order to derive the mathematical model:

B1) Steady state operation.
B2) No heat loss to surroundings.
B3) No heat exchange on the direction of flow.
B4) Plug-flow inside the channels.
B5) Uniform distribution of flow through the channels of a pass.
B6) Perfect mixture of fluid in the end of a pass.
B7) Fluids with Newtonian behavior.
B8) No phase changes.

The fluid inside a channel exchanges heat with the neighbor channels through the thin metal plates, as shown in Fig. (5). The effective heat exchange area is $A = \Phi.w.L$, where Φ is the area enlargement factor, which accounts for the corrugation wrinkles. The length of the path x and the fluid temperature $T(x)$ can be converted into dimensionless form as shown in Eqs (1) and (2).

$$\eta(x) = \frac{x}{L} \qquad 0 \le \eta \le 1 \tag{1}$$

$$\theta_i(T_i) = \frac{T_i - T_{c,in}}{T_{h,in} - T_{c,in}} \qquad 0 \le \theta \le 1 \tag{2}$$

Applying the energy balance to the control volume shown in Fig. (5) (McKillop & Dunkley, 1960) it is possible to derive the differential equations for the channel temperature (Eqs 3, 4 and 5). The overall heat transfer coefficient U_i between channels *i* and *i+1* is given by Eq. (6) as a function of the fluid convective heat transfer coefficient *h*, the plate thermal conductivity k_P and the fouling factor *R* for hot and cold streams.

The mass flow rate inside channel *i* is calculated by Eq. (7) according to assumption B5, where *side(i)* refers to the side that contains channel *i*. It is known that this assumption may not hold for passes with a large number of channels (Bassiouny & Martin, 1984), but there is no rigorous modeling to this behavior. The flow rates in each side, W^I and W^{II}, are associated to the hot and cold fluid flow rates through the parameter Y_h. The direction of the flow in channel *i* is given by the variable s_i. If the flow follows the direction of η, then $s_i = +1$, otherwise $s_i = -1$.

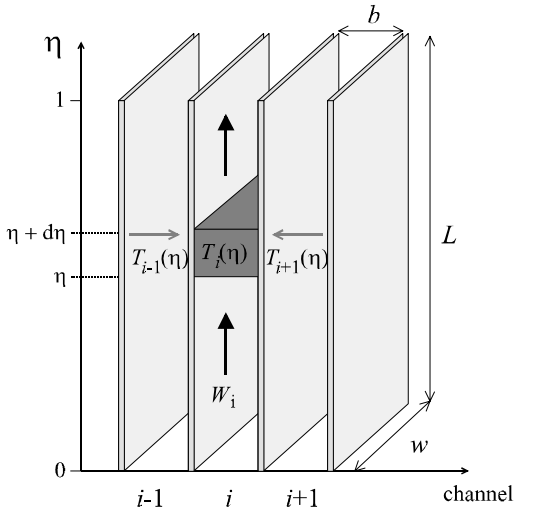

Figure 5. Control volume for derivation of energy balance inside an upward flow channel.

For the first channel:

$$\frac{d\theta_1}{d\eta} = \frac{s_1.A}{W_1.Cp_1}\left[U_1.(\theta_2 - \theta_1)\right] \tag{3}$$

For channel *i*: $(1 < i < N_C)$

$$\frac{d\theta_i}{d\eta} = \frac{s_i.A}{W_i.Cp_i}\left[U_{i-1}.(\theta_{i-1} - \theta_i) + U_i.(\theta_{i+1} - \theta_i)\right] \tag{4}$$

For the last channel:

$$\frac{d\theta_{N_C}}{d\eta} = \frac{s_{N_C}.A}{W_{N_C}.Cp_{N_C}}\left[U_{N_C-1}.(\theta_{N_C-1} - \theta_{N_C})\right] \tag{5}$$

$$\frac{1}{U_i} = \frac{1}{h_i} + \frac{1}{h_{i+1}} + \frac{\varepsilon_P}{k_P} + R_h + R_c \qquad i = 1,\ldots(N_C - 1) \tag{6}$$

$$W_i = \frac{W^{side(i)}}{N^{side(i)}} \qquad i = 1,\ldots N_C \qquad side(i) = \{\mathrm{I}, \mathrm{II}\} \tag{7}$$

The overall heat transfer coefficient is a function of the fluid temperature in the channels (Eq. 6), which depends on η. Since this makes U_i also a function of η, the solution of the system of differential Eqs (3), (4) and (5) is not simple. However, if the fluid physical properties are assumed constant, Eq. (4) can be simplified to Eq. (8), where the coefficients α^I and α^{II} are given by Eq. (9) as a function of the constant overall heat transfer coefficient *U*. Consequently, the system of equations is reduced to a linear system of ordinary differential equations, which is represented in matrix form in Eq. (10), where $\underline{\underline{M}}$ is a tridiagonal matrix and $\underline{\theta}$ is the vector of channel dimensionless temperatures $\theta_i(\eta)$. The analytical solution of Eq. (10) was studied by Zaleski & Jarzebski (1973).

$$\frac{d\theta_i}{d\eta} = s_i.\alpha^{side(i)}.(\theta_{i-1} - 2.\theta_i + \theta_{i+1}) \qquad i = 1,\ldots N_C \qquad side(i) = \{\mathrm{I}, \mathrm{II}\} \tag{8}$$

$$\alpha^{side(i)} = \frac{A.U.N^{side(i)}}{W^{side(i)}.Cp^{side(i)}} \qquad i = 1,\ldots N_C \qquad side(i) = \{\mathrm{I}, \mathrm{II}\} \tag{9}$$

$$\frac{d\underline{\theta}}{d\eta} = \underline{\underline{M}}.\underline{\theta} \tag{10}$$

The necessary boundary conditions for the simplified model, defined by Eq. (8), and for the rigorous model, defined by Eqs (3) through (6), are presented in Tab. (4). Every channel requires a boundary condition equation for its inlet temperature. The inlet position of channel *i* is given by the value of s_i. If $s_i = +1$ the inlet is located at position $\eta = 0$, otherwise the inlet is located at $\eta = 1$. The number and structure of the required boundary equations are functions of the configuration parameters.

For the performance evaluation of the heat exchanger, the thermal effectiveness and the pressure drop calculations are needed. Once the system of equations is solved, the thermal effectiveness *E* can be calculated by Eq. (11) using the average value of the fluid specific heats, where W_c and W_h are related to $W^{side(i)}$ by the parameter Y_h.

$$E = \frac{W_h.\overline{Cp}_h.(1 - \theta_{h,out})}{min\left(W_h.\overline{Cp_h}, W_c.\overline{Cp}_c\right)} = \frac{W_c.\overline{Cp}_c.\theta_{c,out}}{min\left(W_h.\overline{Cp_h}, W_c.\overline{Cp}_c\right)} \tag{11}$$

Table 4. Types of thermal boundary conditions for the PHE channels.

Boundary Condition	Equation Form
Fluid entrance: the temperature at the entrance of the first pass is the same as the stream inlet temperature.	$\theta_i(\eta) = \theta_{fluid,in}$, $i \in$ first pass
Changes of pass: there is a perfect mixture of the fluid leaving the channels of a pass, before entering the next one.	$\theta_i(\eta) = \frac{1}{N}.\sum_{\substack{j \in \text{previous} \\ \text{pass}}}^{N} \theta_j(\eta)$, $i \in$ current pass
Fluid exit: the stream outlet temperature results from a perfect mixture of the fluid leaving the last pass.	$\theta_{fluid,out} = \frac{1}{N}.\sum_{\substack{j \in \text{last} \\ \text{pass}}}^{N} \theta_j(\eta)$

The fluid pressure drops at sides I and II, ΔP^I and ΔP^{II}, can be calculated by Eq. (12) that relies on assumptions B7 and B8 (Shah & Focke, 1988; Kakaç & Liu, 1998). The first term in the right-hand side evaluates the friction loss inside the channels, where G_C denotes the channel mass velocity (Eq. 13a). The second term represents the pressure drop for port flow, where G_P is the port mass velocity (Eq. 13b). The last term is the pressure variation due to an elevation change. Since the gravitational acceleration direction is not associated to the vertical dimension η and there is no information on the pump location, this term is always considered. Therefore the pressure drop may be overestimated.

$$\Delta P = \left(\frac{2.f.(L + D_P).P.{G_C}^2}{\rho.D_e} \right) + 1{,}4.\left(P.\frac{{G_P}^2}{2.\rho} \right) + \rho.g.(L + D_P) \qquad \text{for sides I and II} \qquad (12)$$

$$G_C = \frac{W}{N.b.w} \quad , \quad G_P = \frac{4.W}{\pi.{D_P}^2} \qquad \text{for sides I and II} \qquad (13)$$

The necessary constitutive equations for the calculation of convective coefficients and friction factor, according to assumption B7, are presented in Tab. (5), as well as the necessary dimensionless numbers and the channel equivalent diameter D_e. Usual values for the empirical parameters a_1 to a_6 of the constitutive equations can be found on Saunders (1988) and Shah & Focke (1988).

Table 5. Equations for convective coefficients and friction factor calculation, for sides I and II.

Constitutive Equations	Dimensionless Numbers	Equivalent Diameter
$Nu = a_1.Re^{a_2}.Pr^{a_3}.\left(\frac{\mu}{\mu_w}\right)^{0,17}$ $f = a_4 + \frac{a_5}{Re^{a_6}}$	$Nu = \frac{h.D_e}{k}$, $Re = \frac{G_C.D_e}{\mu}$ $Pr = \frac{C_P.\mu}{k}$	$D_e = \frac{4.b.w}{2.(b + w.\Phi)} \approx \frac{2.b}{\Phi}$

5. Simulation of the PHE

The mathematical modeling of a PHE, for the calculation of its thermal effectiveness and fluid pressure drops, was presented in the previous section. However, it is not possible to derive a model that is explicitly a function of the configuration parameters, especially because of the binary variable s_i and of the required boundary conditions (the equations in Tab. 4).

To overcome this limitation, the modeling was developed in the form of an "assembling algorithm". Given the configuration parameters, this algorithm guides the construction of the complete mathematical model of the PHE and its simulation at steady state operation.

In this work, the solution of the system of equations is carried out by the software gPROMS (Process Systems Enterprise, 2001), using the second order centered finite difference method. In this method, all variables depending on the plate length η are discretized with respect to this dimension. Several schemes were tested and, with 20 discretization intervals within η = [0,1], an excellent approximation of the analytical result was achieved.

The simplified model that relies on the assumption of constant overall heat transfer coefficient and the rigorous model developed by relaxing this assumption were tested and compared. The main structure of the assembling algorithm for the simplified model is presented in Fig. (6). The algorithm has 14 steps as follows:

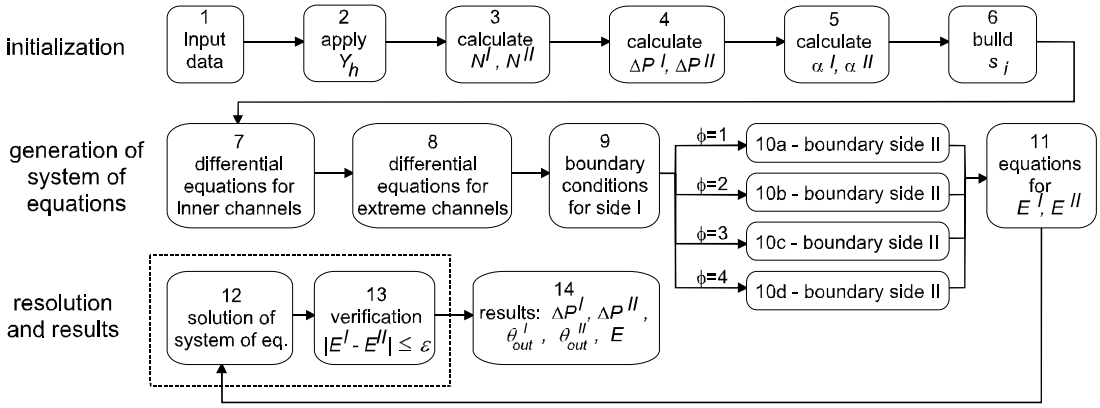

Figure 6. Main structure of the model assembling algorithm.

1) The required data for the PHE (L, w, b, D_P, ε_P, Φ, k_P), for the hot and cold fluids (T_{in}, W, ρ, μ, C_P, k, R, a_1,… a_6) and the configuration parameters (N_C, P^I, P^{II}, ϕ, Y_h, Y_f) are read.
2) The parameter Y_h assigns all fluid data to sides I and II.
3) Numbers of channels per pass N^I and N^{II} are calculated depending on the value of N_C (see Tab. 2).
4) Pressure drops are calculated for both sides of the PHE with Eqs (12), (13) and the equations in Tab. (5).
5) Coefficients α^I and α^{II} are obtained by Eq. (9), using the constant overall heat transfer coefficient U, which is obtained from Eq. (6) using constant heat transfer coefficients for sides I and II, h^I and h^{II}.
6) The values of s_i (i = 1,…N_C) are determined. These depends on the configurations parameters N_C, P^I, P^{II} and ϕ.
7) The assembling of the system of equation starts with the differential equations for the PHE inner channels (Eq. 8).
8) Differential equations for the temperature in the first and last channels are included in the system.
9) Boundary conditions for the channels in side I are generated in the format shown in Tab. (4). The fluid path inside the exchanger, from inlet to outlet, needs to be followed in order to determine the connections between channels.
10) Boundary conditions for side II are also generated, but each value of the parameter ϕ requires a specific treatment because this parameter determines the flow direction inside channels.
11) Equations of thermal effectiveness for both sides (E^I and E^{II}) are included in the dimensionless form of Eqs (14a) and (14b), which are obtained using Eqs (9) and (11).

$$E^I = \frac{N^I}{\alpha^I}.max\left(\frac{\alpha^I}{N^I},\frac{\alpha^{II}}{N^{II}}\right)\left|\theta_{in}-\theta_{out}\right|^I \quad , \quad E^{II} = \frac{N^{II}}{\alpha^{II}}.max\left(\frac{\alpha^I}{N^I},\frac{\alpha^{II}}{N^{II}}\right)\left|\theta_{in}-\theta_{out}\right|^{II} \tag{14}$$

12) The resulting system of differential equations, defined by the differential equations on the temperature in each channel, the boundary conditions equations and the effectiveness equations, is solved by numerical or analytical methods.
13) If a numerical solution method is used, the overall energy conservation can be verified by the effectiveness values E^I and E^{II}. If $|E^I - E^{II}| > \varepsilon$, where ε is the maximum allowable deviation, the parameters of the numerical method and/or the input data should be revised.
14) The main simulation results, such as the pressure drops and outlet temperatures for sides I and II (which are assigned to the hot and cold streams using Y_h), as well as the PHE thermal effectiveness, are obtained.

A computer program was developed to run steps 1 through 11 of the assembling algorithm in Fig. (6). After reading the data, the program makes all necessary calculations, generates a report and creates the formatted input file for gPROMS. This procedure made the simulation of different configurations much simpler and effective.

The derivation of the assembling algorithm for the rigorous model is straightforward. Step 5 should be removed and all the necessary equations for the calculation of the channel overall heat transfer coefficient U_i (Eq. 6), such as dimensionless numbers, constitutive equations and the fluid physical properties dependence upon channel temperature, should be inserted in steps 7 and 8. Equation (14) should also be written in the form of Eq. (11) for the effectiveness calculation in step 11. These modifications increase the size and complexity of the system of equations and make the solution more difficult because of the larger number of discretized variables.

6. Simulation Example

An example of a PHE application is presented to show the simulation results. A hot stream of toluene exchanges heat with a cold stream of benzene in a medium-sized PHE with 25 plates (see Fig. 7). Both rigorous and simplified models were simulated and the main results are presented in Tab. (6) and Figs (8), (9) and (10). For the simplified model, the fluid average temperatures were estimated targeting a thermal effectiveness of 90%.

Table 6. Main simulation results for the example

Variable	Rigorous Model	Simplified Model	Deviation (%)
PHE thermal effectiveness (%)	85.8	86.1	0.35
Benzene outlet temp. (°C)	51.3	51.3	0.00
Toluene outlet temp. (°C)	23.9	23.8	0.42
Benzene pressure drop (kPa)	30.2		-
Toluene pressure drop (kPa)	39.0		-
Number of variables after discretization	4,527	508	-
CPU time on workstation (s)	1.4	0.1	-

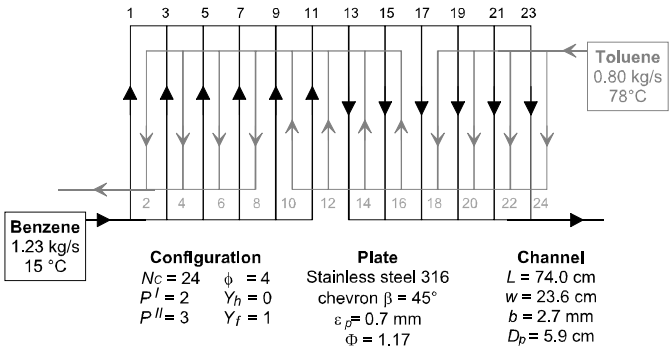

Figure 7. Characteristics of the PHE used for simulation example

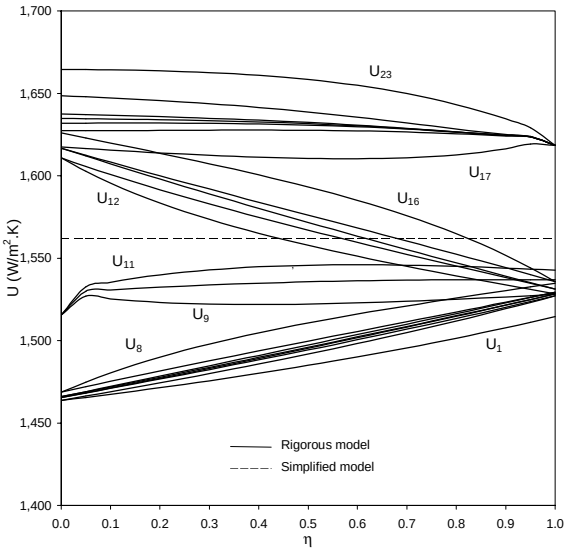

Figure 8. Distribution of the overall heat transfer coefficient along the exchanger

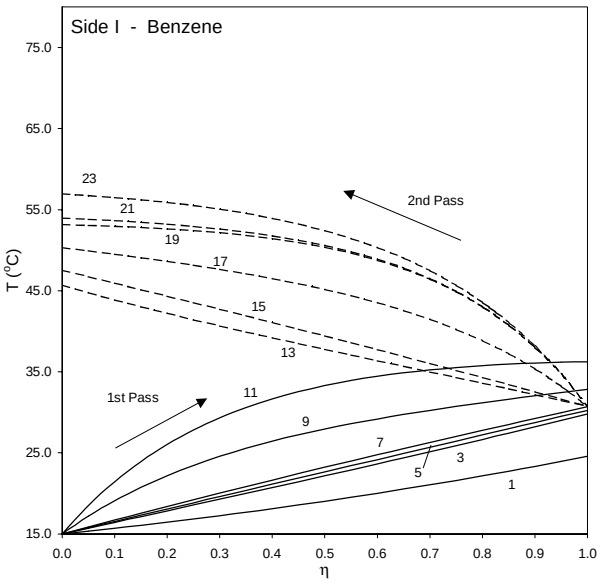

Figure 9. Temperature profiles for side I channels (rigorous model)

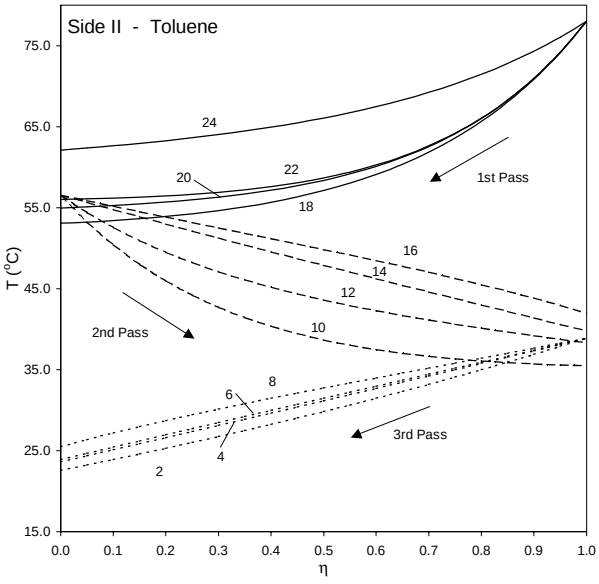

Figure 10. Temperature profiles for side II channels (rigorous model)

The temperature distribution along the exchanger, obtained by the rigorous model, is shown in Figs (8) and (9), where the stream passes and channel numbers are indicated. The temperature variation in the outer channels 1 and 24 are lower than in the other channels in the same pass because heat is exchanged with only one neighbor channel.

The distribution of the overall heat transfer coefficient *U* along the exchanger, obtained by both models, is presented in Fig. (8). The results from the rigorous model simulation showed that the coefficient *U* varies from 1,464 to 1,665 W/m^2.K, while the simplified model was solved with an average value of 1,562 W/m^2.K. Despite this significant

difference, the main simulation results obtained by both models are very close (Tab. 6), with a deviation of only 0.35% for the exchanger effectiveness.

Several examples have shown that, even with a remarkable difference in the distribution of the overall heat transfer coefficient, there is little difference between the main simulation results obtained from both rigorous and simplified models. The obtained deviations were under 1.5%, with respect to *E*.

The number of variables after the discretization by the finite difference method is approximately 9 times larger for the rigorous model. To make the solution of large exchangers reliable, the "block decomposition" option of gPROMS is used, where the system of equations is decomposed into smaller systems. Even with this option, the solution of large exchangers (e.g. 150 plates) using the rigorous model requires 3 to 15 min in a DEC-UNIX workstation. For the case of smaller exchangers, as the one presented in this paper, the solution is achieved in a matter of seconds (Tab. 6).

7. Conclusions

The configuration of a plate heat exchanger (PHE) was characterized by a set of six parameters and a methodology to detect equivalent configurations was presented. Based on this parameterization, a detailed model for the simulation of a PHE in steady state with a general configuration was developed in algorithmic form. The developed assembling algorithm made the simulation and comparison of different configurations more flexible. An important feature of the proposed algorithm is that it may be coupled to any procedure to solve the system of differential and algebraic equations.

The assumption of constant overall heat transfer coefficient along the exchanger, often used for the mathematical modeling, was tested and showed little influence over the main simulation results for heat exchange (thermal effectiveness and outlet temperatures).

The presented algorithm is an important tool for the study of the influence of the configuration over the exchanger performance, and can be further used to develop an optimization method for selecting the pleat heat exchanger configuration. A research in this subject is currently in development.

8. Acknowledgments

The authors would like to thank the financial support from FAPESP (grants 98/15808-1 and 00/13635-4).

9. References

Bassiouny, M.K.; Martin, H., "Flow Distribution and Pressure Drop in Plate Heat Exchangers - I, U-Type Arrangement", Chemical Engng Science, v.39, n.4, pp.693-700, 1984.

Buonopane, R.A.; Troupe, R.A.; Morgan, J.C., "Heat Transfer Design Method for Plate Heat Exchangers", Chemical Engng Progress, v.57, n.7, pp.57-61, July 1963.

Georgiadis, M.C.; Rotstein, G.E.; Macchietto, S., "Modeling and Simulation of Complex Plate Heat Exchanger Arrangements under Milk Fouling" Computers & Chem. Engng, v.22 supS, March/April, pp.S331-S338, 1998.

Kakaç, S.; Liu, H., "Heat Exchangers: Selection, Rating and Thermal Design", CRC Press, New York, 1998.

Kandlikar, S.G.; Shah, R.K., "Multipass Plate Heat Exchangers - Effectiveness-NTU Results and Guidelines for Selecting Pass Arrangements", ASME Journal of Heat Transfer, v.111, pp.300-313, 1989a.

Kandlikar, S.G.; Shah, R.K., "Asymptotic Effectiveness-NTU Formulas for Multipass Plate Heat Exchangers", ASME Journal of Heat Transfer, v.111, pp.314-321, 1989b.

Masubuchi, M.; Ito, A., "Dynamic Analysis of a Plate Heat Exchanger System", Bulletin of the JSME, v.20, n.142, pp.434-441, April 1977.

McKillop, A.A.; Dunkley, W.L., "Plate Heat Exchangers: Heat Transfer", Industrial and Engng Chemistry, v.52, n.9, pp.740-744, Sept. 1960.

Pignotti, A.; Tamborenea, P.I., "Thermal Effectiveness of Multipass Plate Exchangers", Int. Journal of Heat and Mass Transfer, v.31, n.10, pp.1983-1991, Oct. 1988.

Process Systems Enterprise Ltd, "gPROMS Introductory User Guide", Release 2.0, London, 2001.

Saunders, E.A.D., "Heat Exchangers: Selection, Design & Construction", Longman S.&T., New York, 1988.

Settari, A.;Venart, J.E.S., "Approximate Method for the Solution to the Equations for Parallel and Mixed-Flow Multi-Channel Heat Exchangers", Int. Journal of Heat Mass Transfer, v.15, pp.819-829, 1972.

Shah, R.K.; Focke, W.W., "Plate Heat Exchangers and their Design Theory", in: Shah, R.K.; Subbarao, E.C.; Mashelkar, R.A., Editors, "Heat Transfer Equipment Design", pp.227-254, Hemisphere P.C., New York, 1988.

Taborek, J., "Shell-and-tube Heat Exchangers: Single-phase Flow", in: Hewitt, G.F., Editor, "Handbook of Heat Exchanger Design", s.3.3, Begell House, New York, 1992.

Zaleski, T., "A General Mathematical-Model of Parallel-Flow, Multichannel Heat-Exchangers and Analysis of its Properties", Chemical Engng Science, v.39, n.7/8, pp.1251-1260, 1984.

Zaleski, T.; Jarzebski, A.B., "Remarks on Some Properties of Equation of Heat-Transfer in Multichannel Exchangers", Int. Journal of Heat Mass Transfer, v.16, n.8, pp.1527-1530, 1973.

Zaleski, T.; Klepacka, K., "Approximate Methods of Solving Equations for Plate Heat-Exchangers", Int. Journal of Heat Mass Transfer, v.35, pp.1125-1130, 1992.